International Journal of Innovative Research and Scientific Studies, 8(1) 2025, pages: 81-93

IJIRSS
International Journal of Innovative Research & Scientific Studies

ISSN: 2617-6548

URL: www.ijirss.com

Experimental studies of sensors based on fiber Bragg gratings embedded in the internal structure of composite plates

Aliya Kalizhanova[1], Ainur Kozbakova[2*], Murat Kunelbayev[3], Beibut Amirgaliyev[4], Zhalau Aitkulov[5]

[1]*Institute of Information and Computer Technologies CS MSHE RK, Almaty University of Energy and Communications named after G. Daukeyev, Kazakhstan.*
[2]*Institute of Information and Computer Technologies CS MSHE RK, Almaty Technological University, Kazakhstan.*
[3]*Institute of Information and Computer Technologies CS MSHE RK, Kazakhstan.*
[4]*Astana IT University, Astana, Kazakhstan.*
[5]*Institute of Information and Computer Technologies CS MSHE RK, Kazakh National Women's Teacher Training University, Kazakhstan.*

Corresponding author: Olanrewaju, Kofoworola Misturat (*Email: ainur79@mail.ru*)

Abstract

The main purpose of this article is to study the structural characteristics of carbon fiber samples printed on a 3D printer, including embedded sensors, during 3D printing, through numerical and experimental studies. There is a widespread tendency to replace metals with modern composite materials. Various methods can be used to measure the destruction of the composite structure. Fiber Bragg array sensors are known as intelligent localized and global structural condition prediction devices for all kinds of structural applications, especially those using composite materials. In this work, we created control plates by impregnating a selected number of layers of carbon fabric with epoxy resin. Fiber-optic Bragg sensors were additionally located between the layers of carbon fabric. In the course of experimental studies, a fiber Bragg grating sensor was embedded in the middle of the sample, and a second sensor was attached to the finished surface of the sample. We conducted environmental tests to examine the durability of the additively manufactured standard's components and the impact of integrated sensors on the composite sample. We applied the concept of equations, known as conjugate modes, and used the transition matrix method to solve them numerically. The scientific novelty of the work is the development of a new method and technology for measuring spatial deformation in composite materials using fiber-optic Bragg gratings.

Keywords: Additively manufactured standard, Carbon fiber, Composite material, Fiber optic sensor, Transition matrix method, 3D printing.

DOI: 10.53894/ijirss.v8i1.3574
Funding: This research is supported by the Science Committee of the Ministry of Science and Higher Education of the Republic of Kazakhstan (Grant number: AP 19679153).
History: Received: 8 January 2024/**Revised:** 5 August 2024/**Accepted:** 2 September 2024/**Published:** 4 October 2024

Competing Interests: The authors declare that they have no competing interests.
Authors' Contributions: All authors contributed equally to the conception and design of the study. All authors have read and agreed to the published version of the manuscript.
Transparency: The authors confirm that the manuscript is an honest, accurate, and transparent account of the study; that no vital features of the study have been omitted; and that any discrepancies from the study as planned have been explained. This study followed all ethical practices during writing.
Institutional Review Board Statement: The Ethical Committee of the Institute of Information and Computational Technologies CS MSHE RK, Kazakhstan has granted approval for this study on 3 August 2023 (Ref. No. 298/23-25).
Publisher: Innovative Research Publishing

1. Introduction

The development of modern technologies is aimed at increasing the safety and reliability of the design, taking into account the needs of energy savings and environmental protection. There is a widespread tendency to replace metals with modern devices. The undeniable advantage of composite materials is their high strength and relatively low weight. That is why interest in composite materials among companies in the construction, aviation, and automotive, medical, information, communications, and manufacturing industries is very high.

The destruction of a composite structure can be measured by various methods. People often use ultrasound or X-ray methods. Such measurements usually take several hours. They may be linked to the structure's decommissioning and financial losses.

Currently, a significant percentage of composite materials in aircraft construction is an indicator of their innovation and demand.

Industries such as space technology, aircraft, shipbuilding, and automotive use composite fibrous materials extensively. The use of composite materials in modern structures provides significant gains in weight, strength, durability, resistance to corrosion, and aggressive chemical environments. These materials also serve as excellent substitutes for metals. Thus, of the total volume of polymer materials consumed in the United States to replace metals, 40-50% are used for the manufacture of car parts, instruments, calculating machines, and other general engineering products; 30-35% are used for the manufacture of pipes, fittings, and profiles; 10-15% are used ship hulls, aircraft, and missile parts.

Various methods can measure the degree of degradation of the composite structure. People often used ultrasound or X-ray methods. Such measurements usually take several hours. They may be associated with the structure's temporary exclusion from normal use and financial losses. Fiber optic sensors are another method that makes it possible to study the degree of degradation of the composite structure and the influence of parameters such as strain and temperature. The undeniable advantage of their use is the fast and structure-safe measurement of physical quantities. Measurements can be made during the structure's operation. Fiber optic sensors can be placed inside the composite material or glued to its surface. The concept of placing fiber optic sensors inside a composite material is known as smart structure. Finding an optimal method for controlling a structure's degradation rate will extend the life of its operation. Several types of optical fiber sensors can be housed in a composite structure. The classification can be based on the location of optical signal processing-external and internal. Fiber optics in externally processed sensors performs the function of sending and removing light into and out of the sensor, where the measured value information is processed. This category includes edge sensors, gear shift sensors, and diffraction gratings. In these types of sensors, light modulation occurs outside the optical fiber. In internally processed sensors, the optical fiber additionally acts as an optical converter.

In the literature reviews, Gebremichael, et al. [1]; Mieloszyk, et al. [2]; Cucinotta, et al. [3] and Liu, et al. [4] have developed fiber Bragg grating sensors that are used in systems to predict the condition of systems installed in various composite structures. In system health prediction systems of Wu, et al. [5] and Chen, et al. [6] FBG sensors are used to measure voltage and temperature. The advantages of FBG sensors, such as their small size and weight, multiplexability, and corrosion resistance, allow them to be integrated into complex structures, such as composite structures, as in the case of aircraft cabins [7]. The mechanical and geometric parameters of FBG sensors have a limited impact on material reliability.

Currently, composite materials are produced using 3D printing. Layer by layer, these manufacturing process deposits successive layers of material using computer-aided design to form the final product. is done layer by layer, where layers of material are deposited successively using computer-aided design to form the final product. It is widely used in various industries, such as aviation and automotive, to produce special parts, especially those with complex geometries. 3D printing provides unsurpassed elasticity for the product compared to classical production technologies. Parandoush and Lin [8] investigated 3D-printed composite material to improve plant performance while significantly reducing environmental impact. On the other hand, the demand for composite materials has increased significantly over the past few years. A trend was explored in Guo, et al. [9] which is largely due to the fact that composite materials have outstanding structural properties that distinguish them from conventional isotropic materials and naked polymers.

Composite materials have an improved stiffness-to-weight ratio, are corrosion resistant, and are thermally stable. The use of 3D printing for the production of continuous fiber reinforced composite materials has increased in recent years by

Yu, et al. [10]; Van De Werken, et al. [11]; Mahmood, et al. [12]; Penumakala, et al. [13]; Chakraborty and Biswas [14], and Kousiatza and Karalekas [15]. Lee, et al. [16]; Zhong, et al. [17]; Ning, et al. [18]; Chacón, et al. [19] and Kabir, et al. [20] carried out precipitation fusion modeling, which seems to be one of most the widely used, free, low surface porosity, and low cost technologies that can still be bonded to thermoplastic materials is still considered a potential candidate for industrial applications. Wu, et al. [5] developed a continuous material winding method integrated into a printing platform. The warm end continuously melts the elastic thread, which a hot nozzle then embeds onto the construction platform. The applied molten substance instantly cools, solidifies, and attaches to adjacent rasters, where during this time a phase transition occurs.

The final material was produced by lifting the melter nozzle upward and placing another shell on top, according to Mieloszyk and Ostachowicz [21]. Over the past decade, an impressive amount of research has been conducted on precipitate fusion technologies for the fabrication of composite materials by Kousiatza, et al. [22]. Sorensen, et al. [23] and Mieloszyk, et al. [24] have fabricated FBG sensors that can be integrated into the PLA material during its production using classical methods. Fernández-Medina, et al. [25] developed CFRP optical hardware that meets stringent conditions for insert placement and very strict constraints on dimensional stability with respect to temperature changes. They fabricated a model of the optical bench that included integrated FBG sensors for temperature and voltage measurements. FBG temperature sensors have been characterized and third-order polynomial calibration has been proposed. We obtained good agreement when comparing temperature measurements using FBG and thermocouple sensors. The deformation of the optical bench was measured using integrated and surface FBG stress sensors, and the results were compared.

Gabardi, et al. [26] successfully integrated FBG sensors into CFRP composite laminates for structural health monitoring. Preliminary mechanical and thermal testing of the laminate with sensors was performed to confirm integration progress. To verify the process's repeatability and validate a new mechanical model to describe the performance of CFRP laminates a s a material with variable tensile or compressive stiffness, tests were conducted using an end slide bending test. The model was validated by independently measuring the equivalent stiffness of the laminates using a laser pointer. The paper by Vedran, et al. [27] presents an optical fiber sensor for detecting corrosion processes on iron surfaces. In the proposed sensor design, an optical fiber coated with a high-order Bragg grating is attached to the observed iron surface. There is an enhancement in the spectrum of the high-order Bragg grating, which is used to detect small and highly localized changes in longitudinal strain starting along the fiber as a result of the formation of corrosion fakes under the sensitive fiber. The proposed approach guarantees simple manufacturing, the possibility of minor installation by starting the construction of the sensor under layers of anti-corrosion coating, and stable consequences of corrosion.

Extensive development of FBGs over the decades has resulted in this type of system becoming one of the most advanced optical fiber technologies for detection, demonstrating superior performance for a very wide range of applications. Polydimethylsiloxane (PDMS) material comes in the form of a microchip, which ensures a dry gecko-like grip for FBG-based non-contact temperature measurement. In addition to providing protection, the PDMS material with an integrated polyamide capillary reduces the mechanical stress transferred to the optical fiber, allowing FBG-based temperature measurements to be performed with minimal deformation effects. Furthermore, the application of the microchip design to one of the packaging planes ensures a dry gecko-type grip through van der Waals forces. This feature allows the enclosed optical fiber sensor to be suspended and detached from virtually any smooth surface without leaving fingerprints on the monitored structure. The study's results indicate that the sensor responds quickly and accurately to temperature, with a significantly reduced effect of permanent deformation.

The proposed packaged sensor can be used in cases where the use of adhesive is prohibited or not recommended by Shuochao, et al. [28]. Quattrocchi and Montanini [29]discuss the development of a visual self-detection structure obtained by incorporating an FBG sensor into a 3D stereolithography (SLA) printing process. The paper describes the strategies employed to ensure a tight fit of the FBG sensor into the structure and the experimental tests used to test the structural resonances of the self-detection structure sample. The study's results demonstrated that the sensitive demonstration structure successfully tested the thermochemical characteristics of the additive manufacturing (AM) process, ensuring accurate strain identification and measurement under controlled stress.

The main objective of this study is to investigate the structural performance of 3D-printed CFRP samples, including embedded FBG sensors, during 3D printing through numerical and experimental studies. It should be noted that, unlike traditional attachment methods, when using epoxy resin to attach the FBG sensors to the CFRP samples, they attached naturally during the 3D printing process in such a way that no peeling occurred.

2. Research Methodology

We made control plates in this work by impregnating a selected number of layers of carbon fabric with epoxy resin. Fiber-optic Bragg sensors were additionally located between the layers of carbon fabric. Technical characteristics of the carbon fabric used to prepare the control plates: 200g/m2, 0.15–0.30mm.

The epoxy resin was mixed with the hardener in a 2:1 ratio and moderately divided each layer of carbon fabric with a brush. Layers impregnated with a suitable amount of carbon fiber were placed between two glasses, which made it possible to isolate the finished plate from the glass relatively freely.

The glass panels between which the control board was located were pressed together, which ensured that air bubbles were squeezed out of the structure. Additionally, we gave the slabs a smooth top surface. Figure 1 shows the carbon fiber fabric and epoxy resin used in the plate preparation process.

Figure 1.
Carbon fabric and epoxy resin used to create control plates.

The internal structure of the composite flakes is schematically shown in Figure 2. In addition, the scale of the cut parts of the carbon fabric from which the flakes are formed after wetting and curing is shown.

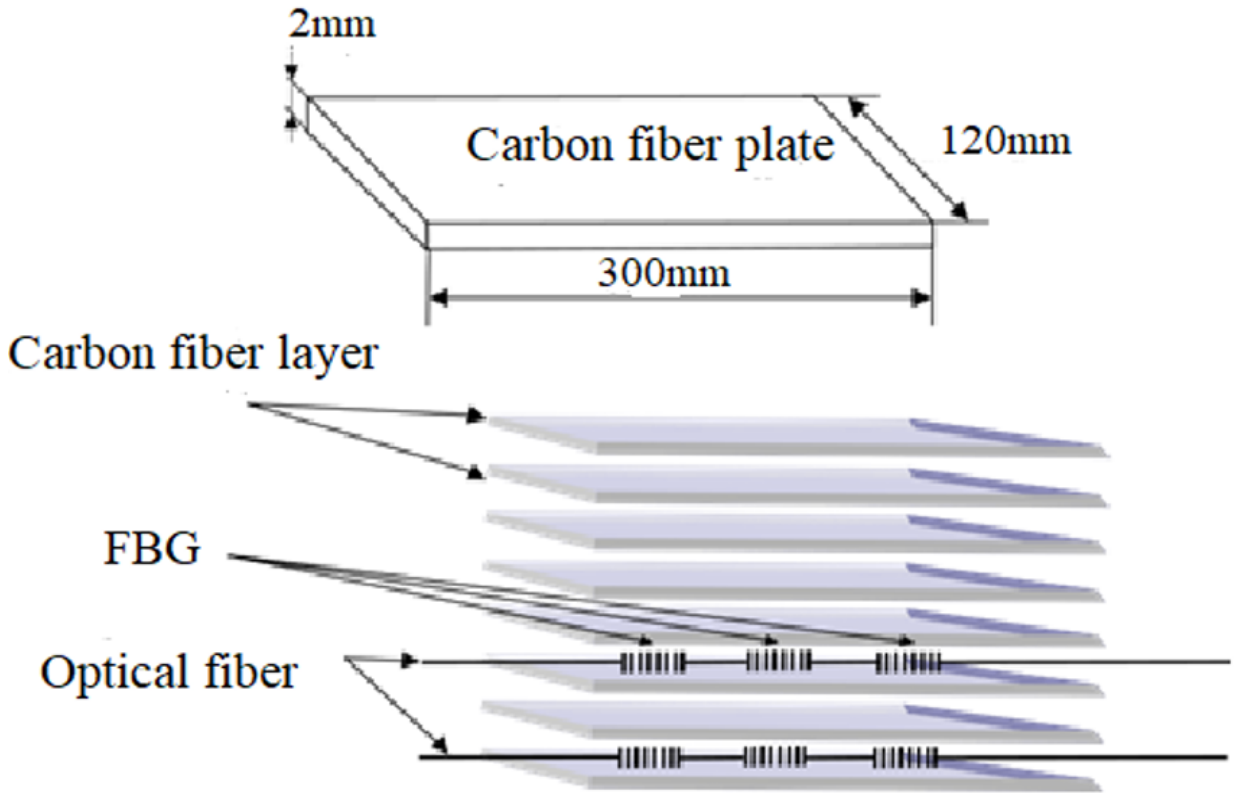

Figure 2.
Internal structure of the proposed control boards with schematically labeled FBG fiber optic sensors.

During the technological processing of preparing samples from a composite material with the fiber, the following tasks were set: selection of technology for establishing the state of the fiber with FBG in the required location and in the required direction; analysis of the appropriate number of Bragg gratings in the sample; establishing the coordinates of the location of each component after preparing the sample; ensuring effortless fiber ends; analysis of the possibility of fibers intersecting with each other; analysis of the ability to place a water diode between sample levels. Figure 3 illustrates the creation of a carbon fabric plate for research purposes.

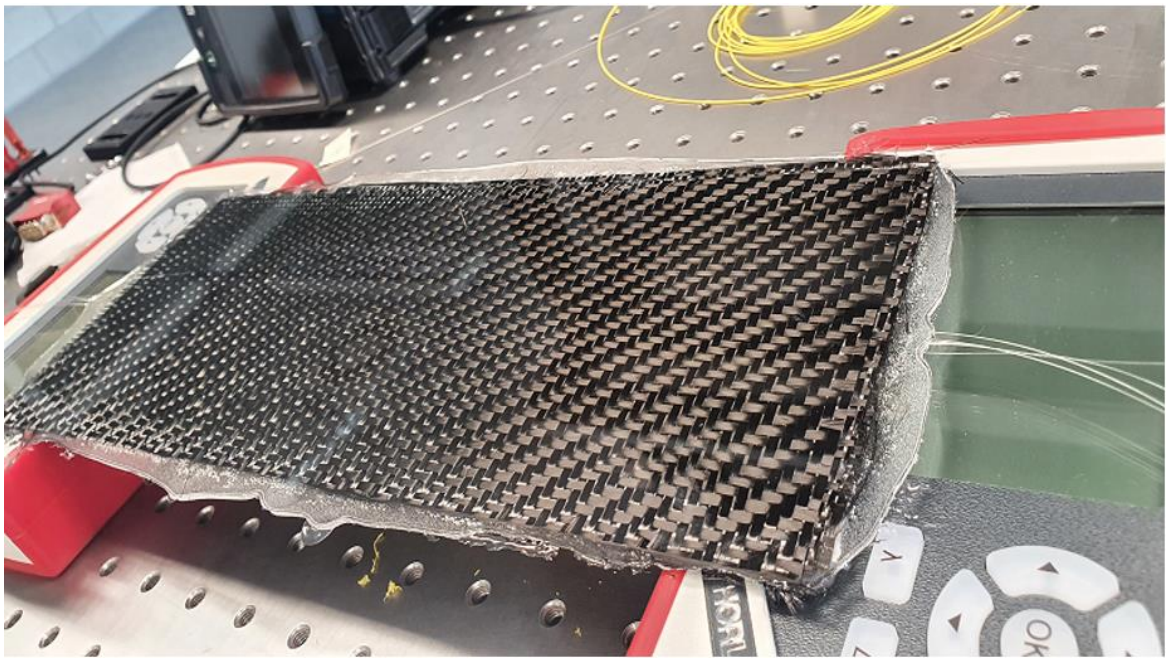

Figure 3.
Plates created for research work.

Method was used to deposit fiber Bragg gratings, which were used to be embedded into the structure of composite plates. A particularly significant component of the system. We used interference mirrors to transmit the laser beam. A cylindrical lens directed the laser beam to the phase mask, focusing it. Photosensitive fiber from THORLABS, sample GF1 with increased germanium content, was placed naturally behind the phase mask. Figure 4 schematically shows the design for preparing periodic fiber-optic structures, equipped in the laboratory of optoelectronics and laser technologies at the Lublin University of Technology.

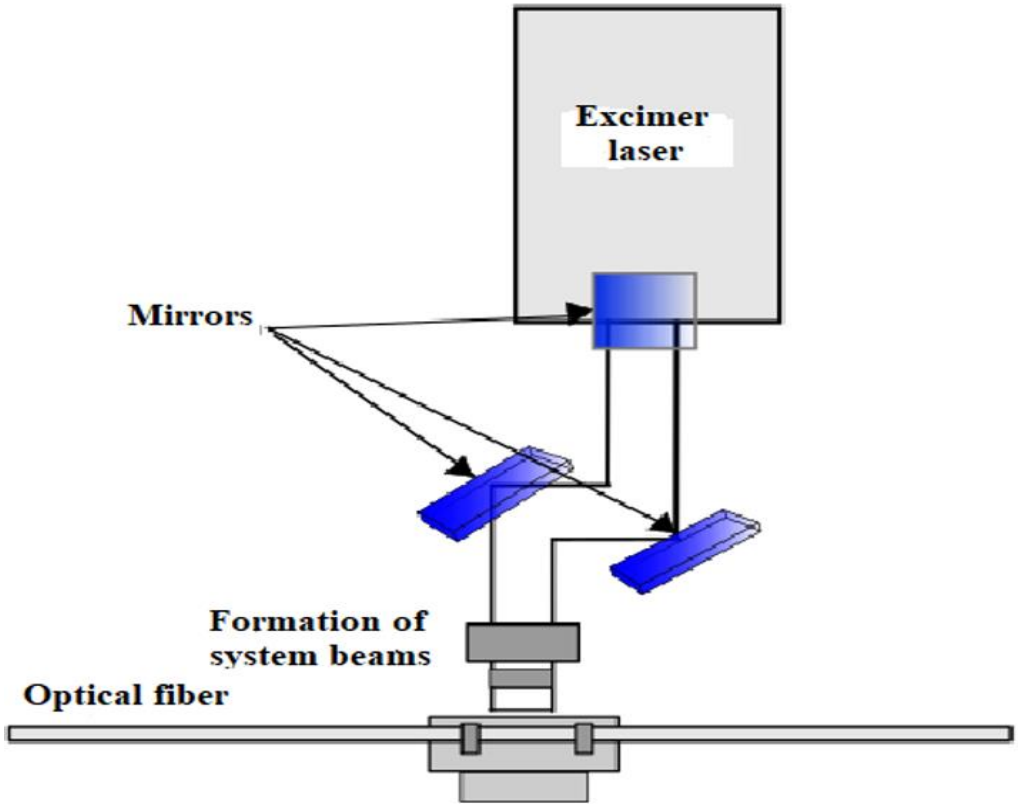

Figure 4.
Diagram of a system for recording periodic fiber structures in the laboratory of optoelectronics and laser technologies.

In the described system, the beam focus was located between a phase mask and an optical fiber (as shown in Figure 4). At high enough laser pulse energies, indenting the lens and forcing the beam focus closer to the surface of the fiber, will initially damage the optical fiber. As a result, tuning system operating parameters near conditions that are risky for

optical components will reduce the risk of damage to the phase mask. Speculative proposals for induced stresses in a material subjected to bending, as presented in Figure 4, indicate that there will be no stresses in the major axis of the plate. We should monitor the material's compression in the upper shell of the slab and tension in the lower one. Figure 5 shows a photo of a real measuring system.

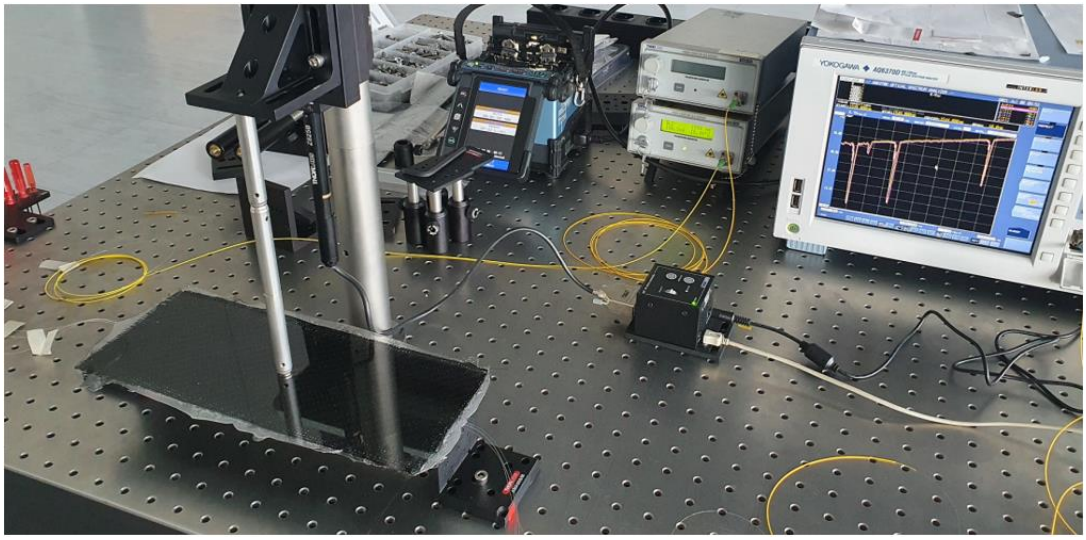

Figure 5.
Measuring system for stress tests in a test plate.

Figures 4 and 5 schematically present the experimental studies conducted in the measuring system. The light source for periodic sensors was an SLED diode THORLABS S 5 FC 1550 S – A 2, whose spectra were measured using a YOKOGAWA optical spectrum analyzer AQ 6370 D.

The first type of periodic structures are FBGs, where the distance between successive modulations Λ (the so-called grating period) is on the order of hundreds of nanometers, and the grating itself operates in the reflection mode. A larger lattice period, on the order of hundreds of micrometers, is characterized by long periodic DPR gratings (LPG) operating in transmission mode [11]. Cladding modes operate in transmit mode due to their high attenuation and rapid disappearance.

The differences in the technological parameters of both types of periodic gratings (modified refractive index -, period - Λ and grating length - *L*, as well as the manufacturing method), are expressed in two different physical phenomena that occur during the propagation of a light beam in a modified fiber, and, consequently, in spectral properties synthetically compared in Table 1.

Table 1.
Comparison of the main parameters and properties of a Bragg grating (FBG) and a long-period fiber grating (LPG).

Properties	**FBG (FBG)**	**DPR (LPG)**
Period Λ	Less than 0.1 mm, usually 0.5 μ m	Between 0.1–1 mm, usually 200–300 μ m
Length L	A few centimeters (2–4cm)	
Pairing mods	Coupling of a core mode propagating in the positive direction (From the source to the second end of the fiber) with a core mode in the opposite direction	Conjugation of core modes propagating in the positive direction with cladding modes also propagating in the positive direction
Spectral characteristic	In the transmission spectrum, there is attenuation for one wavelength that satisfies the phase matching condition (Bragg wavelength)	The transmission spectrum consists of absorption bands for different wavelengths
Sensitivity	There is no sensitivity to changes in the external refractive index of the surrounding area	The ability to obtain ultra-sensitive gratings through modification of boundary conditions. High sensitivity to changes in external Rl.

In general, the lack of connection with cladding modes in the case of FBGs eliminates the possibility of processing the signal coming from changes in the refractive index of the environment.

Induced refractive index modulation within the fiber core provides coupling to multiple cladding modes; thus, part light passes along the fiber cladding and is then absent from the fundamental mode of the core.

As in the case of Bragg gratings, the phase matching condition resulting from the principle of conservation of momentum (PMC, or Phase–Condition), must also be satisfied for LPG so that mode coupling and extinction occur at a selected wavelength. Considering a single-mode fiber with propagation constant β 0.1 for the fundamental modulus and

βpl, (m) for higher order modes (m), the phase matching condition can be expressed as follows:

$$\beta\ 0.1 - \beta\ clad\ (\ m\ )\ =\ \frac{2\pi}{\Lambda}. \qquad (1)$$

From the definition of the propagation constant

$$\beta\ =\ \frac{2\pi}{\lambda} nef, \qquad (2)$$

We obtain the phase matching condition for LPG , expressed by the difference in the effective refractive indices between the base and m-order cladding modes, as:

$$\lambda_{LPG\ (m)} = \Lambda \cdot (\ n_{core}^{eff} - n_{clad,(m)}^{eff}\ ) = \Lambda \cdot \Delta n\ \text{eff}\ , \quad (3)$$

Where: $\lambda_{LPG\ (m)}$ is the resonant wavelength of the absorption band under phase matching conditions, $n_{core}^{eff}$is the effective refractive index of the core, $n_{clad,(m)}^{eff}$is the effective refractive index of the cladding, $n_{core}^{eff}$and $n_{clad,(m)}^{eff}$ are the effective RI of the fundamental mode and the higher order mode (m-order), m is the order of the mode, respectively. It should be noted that the values of $n_{core}^{eff}$and $n_{clad,(m)}^{eff}$ strongly depend on the refractive index of the fiber coren_{core}^{eff} and the refractive index of the fiber cladding $n_{clad,}^{eff}$, which is caused by the dispersion of the waveguide.

Manufacturing technology of long - period fiber optic lattices. Local modulation of the optical fiber core introduced to produce LPG can occur by:

1) optical modulation: a change in the refractive index of the optical fiber core material caused by the introduction of periodic voltages;

2) Geometric modulation: periodic reduction in the diameter of the optical fiber.

The first method requires, in order to sensitize the material to the wavelength of light used, the fiber hydrogenation process underlying LPG. Periodic tapering of the fiber can be accomplished by locally etching the cladding to a specific fiber diameter. The production of LPG by periodic micro-oscillation of the fiber is the cheapest method, requiring a setup for the production of a cone based on: an arc discharge or heating of a fibrous material placed in a welding machine (Ω-shaped tungsten filament).

The production of LPG by reducing the diameter of the optical fiber can be carried out either by partial etching with hydrofluoric acid or by spot micro-compression of the optical fiber. The main difference is in the geometry of the areas of reduced transverse diameter: local etching reduces the diameter of only the fiber cladding (Figure 6a); whereas in the case of microannealing, the diameter of both the fiber core and the fiber cladding decreases (Figure 6b).

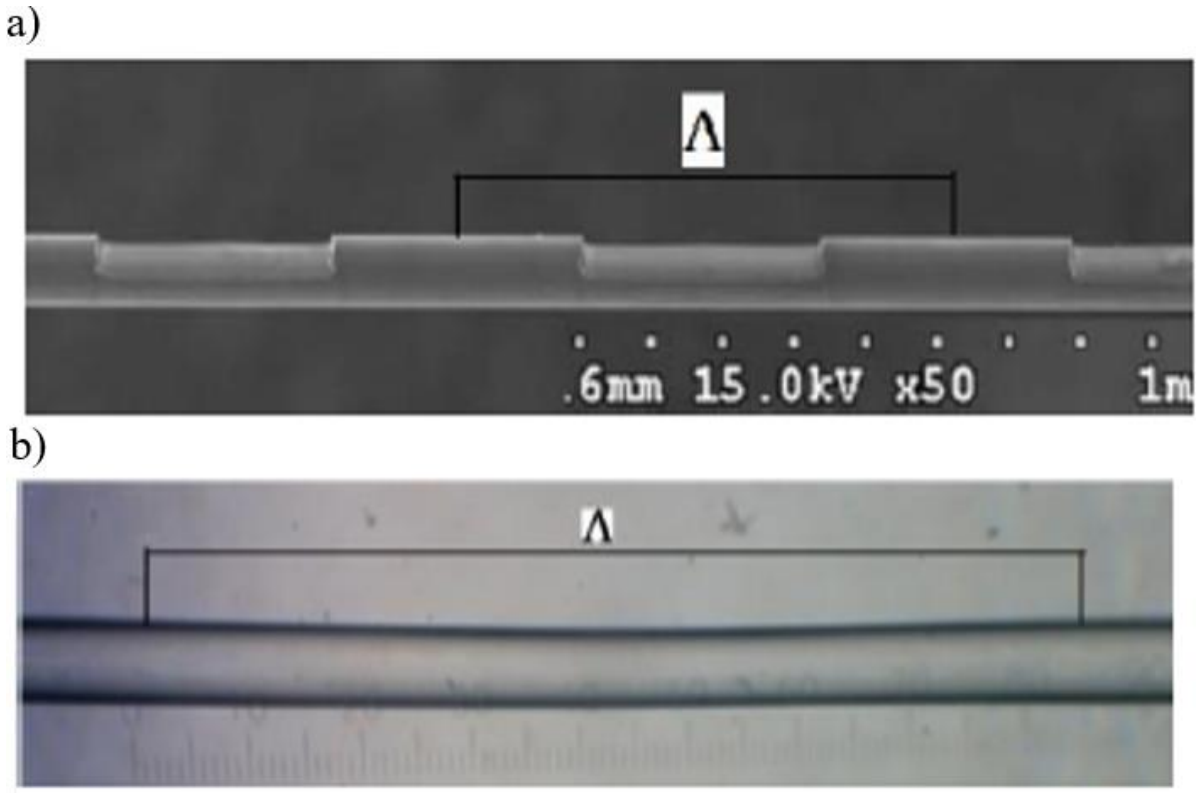

Figure 6.
Schemes of the results of manufacturing LPG gratings: a) Etching, b) Microannealing.

3. Results

Figure 7 shows the spectral characteristics obtained by numerical simulation. To do this, the concept of conjugate mode equations was used, which was solved numerically using the TMM transfer matrix method.

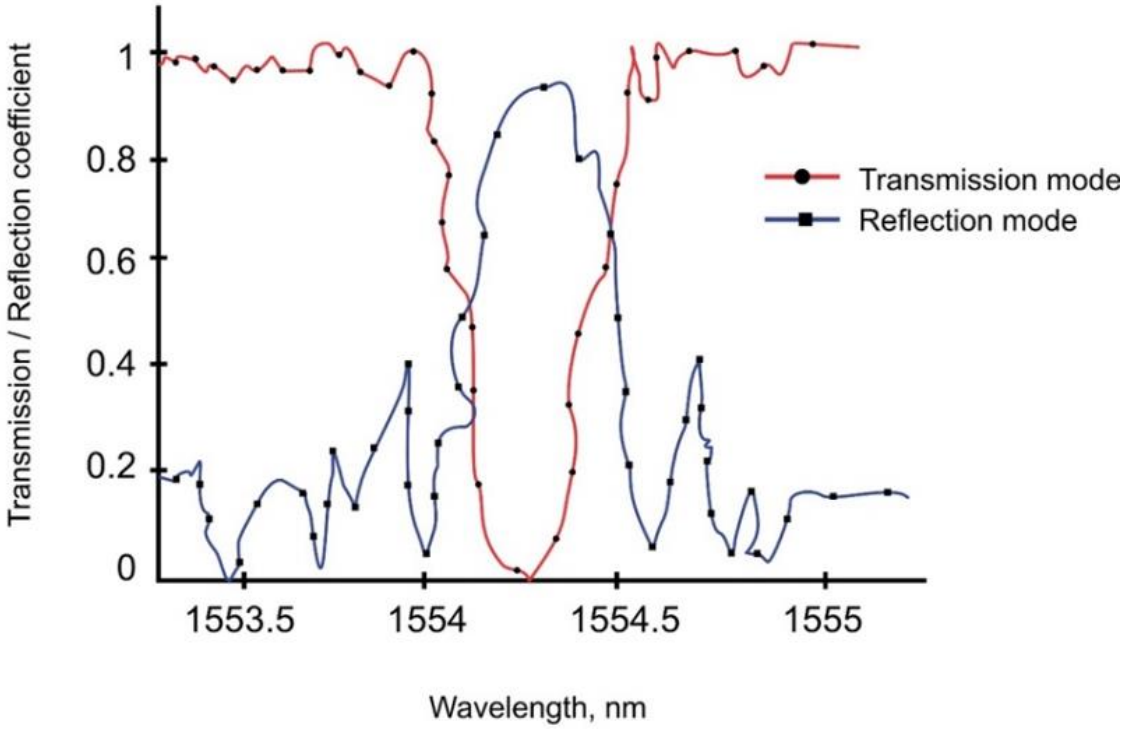

Figure 7.
Characteristics modeled using the transfer matrix method (Transfer matrix method). FBG structure length = 11 mm.

eff = 1.4567 and the grating length were taken to be L = 11 mm. The refractive index modulation depth δaccepted through calculations was n = 0. 00025, which corresponds to the so-called weak lattice. The Bragg wavelength of the designed structure was λB = 155 7. 7nm.

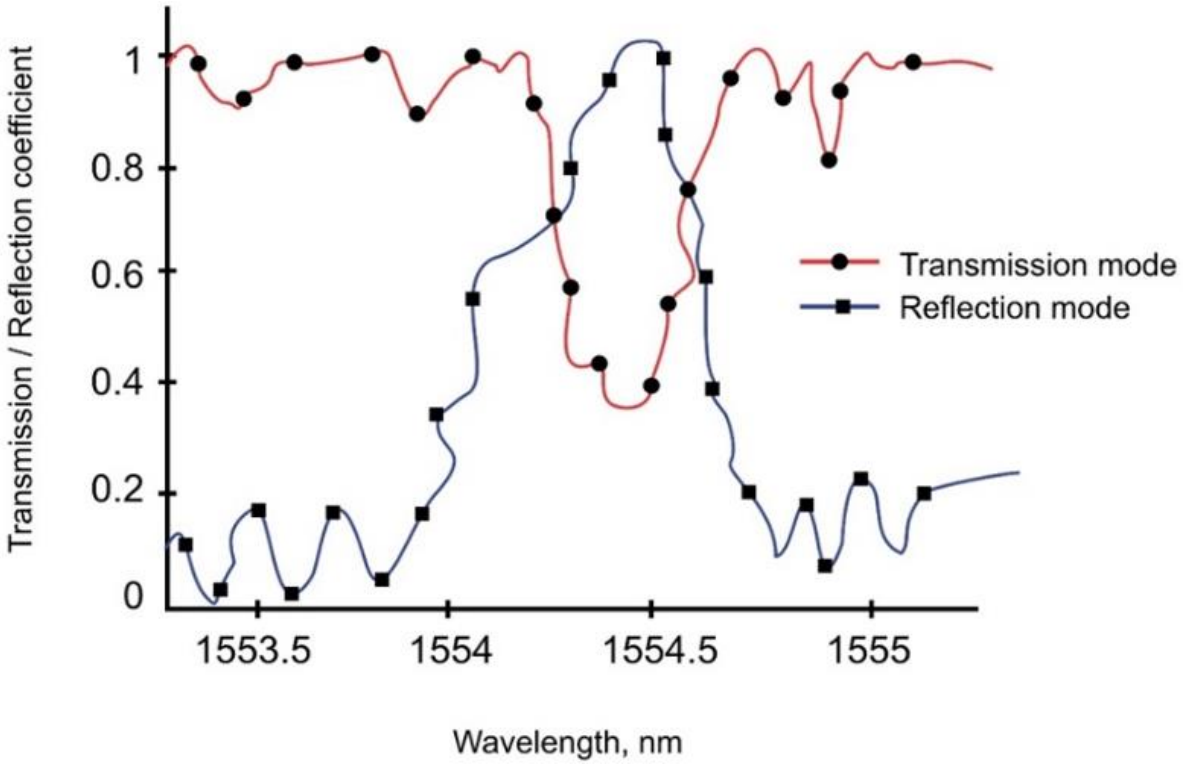

Figure 8.
Characteristics modeled using the transfer matrix method (Transfer matrix method). FBG structure length = 7mm.

Figure 8 shows the spectral characteristics in transmission and reflection modes performed for a structure with a length of 7 mm. The noticeable decrease in reflectivity and transmission values for the central wavelength (Bragg wavelength) is associated with a decrease in the entire's structure length. As you can see, the half width of the calculated characteristics has not changed.

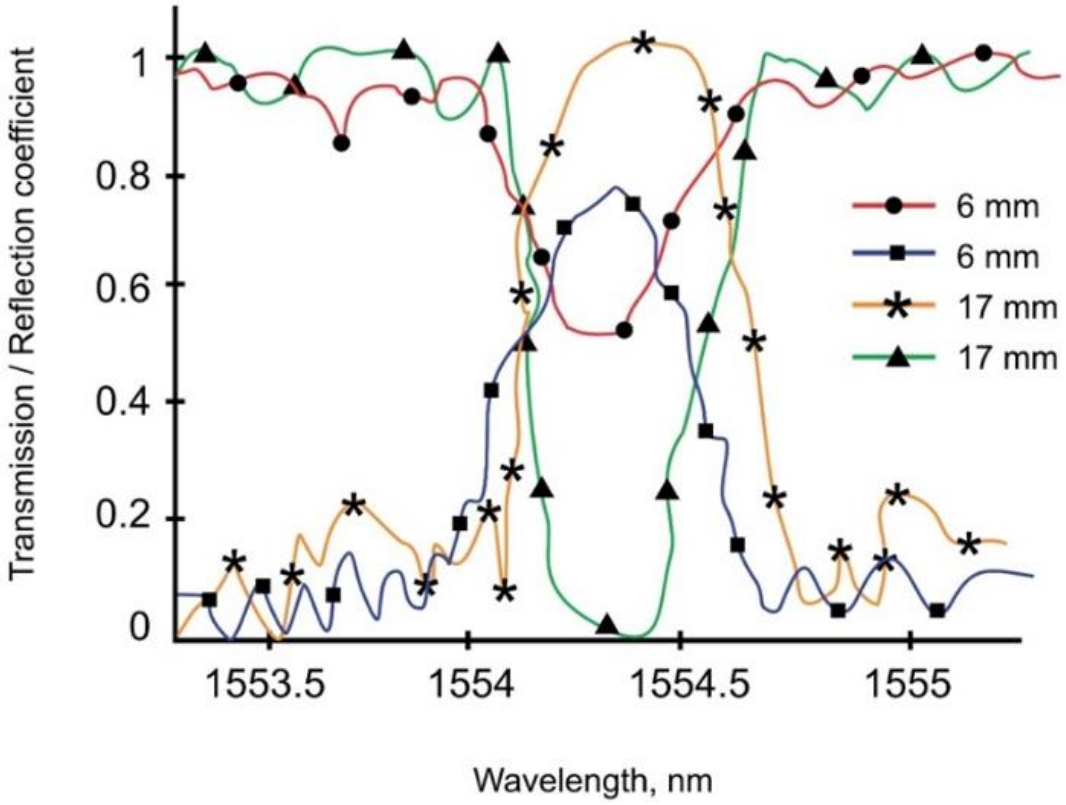

Figure 9.
Shape of spectral characteristics for FBG structure = 6 mm and 17 mm.

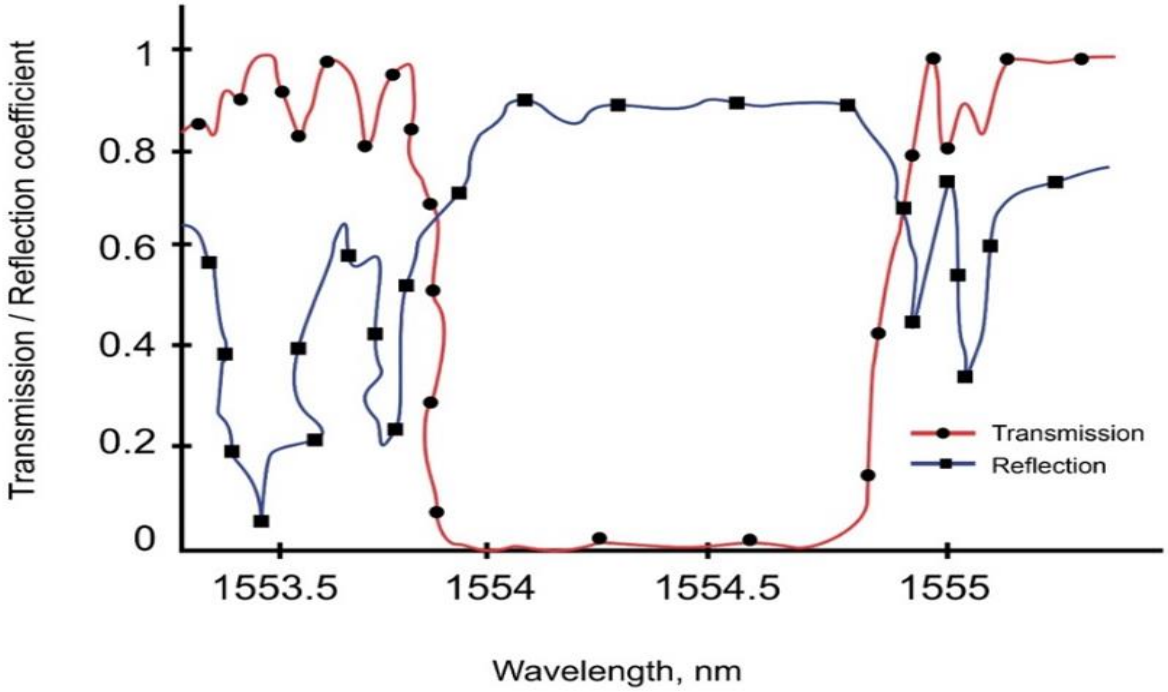

Figure 10.
Shape of spectral characteristics for a structure with a length of 11 mm and a refractive index modulation depth of 0.002.

Figure 9shows the collected reflections and transmissions of an 11-mm-long structure with a refractive index modulation value of δn = 0.002. Characteristically, there is a shift in characteristics and a strong expansion of the half-width of the main transmission and reflection peak of the grating. Structures fabricated in laboratories typically have refractive index modulation variations ranging from 0.0005 to 0.00001. Therefore, Figure 10 collects the transmission spectra of 11-mm-long structures with δ_n values that are in this range.

Figure 11 shows the transfer of the FBG structure for selected values of the refractive index modulation depth. The physical length of the structures is 11 mm, the central wavelength is 1554.8 nm. This figure clearly demonstrates how the reflective index modulation shift influences the half-width and spectral range of the structure's main reflection peak. At lower modulation values, the transmission coefficient also changes significantly. A grating with the refractive index

modulation value of 0.00001 and below practically disappears, and the reflectance for the central Bragg wavelength drops to a value below 0.01.

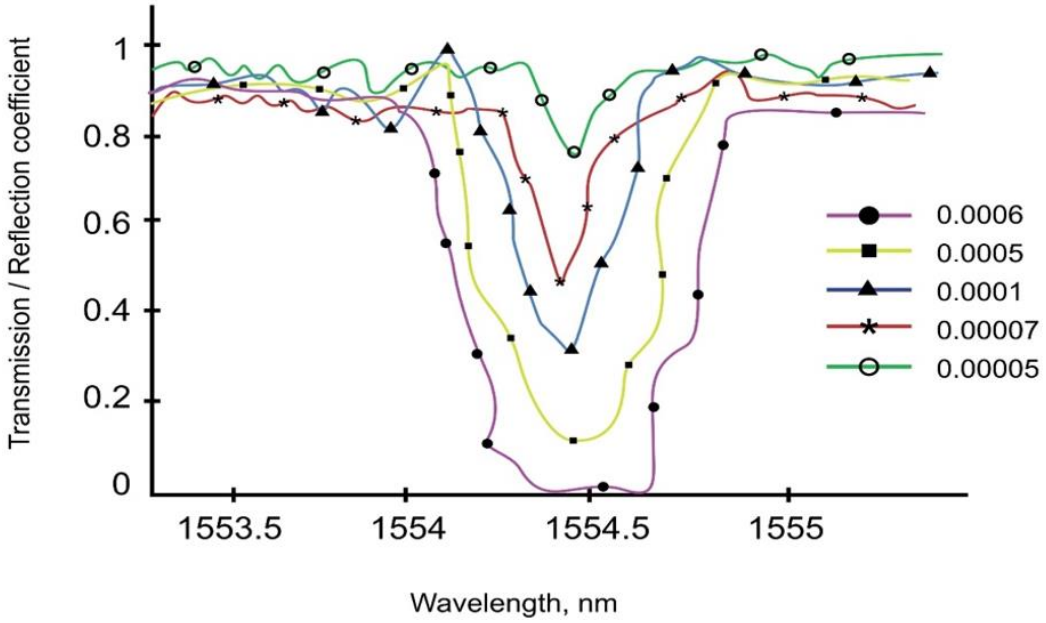

Figure 11.
FBG structure transfer for selected refractive index modulation depths, physical structure length 11 mm, center wavelength equal to 1554.8 nm.

Figures 12, 13, 14 show the results of numerical calculations for structures 17 and 19 mm long for various apodization values. The calculations used a Gaussian apodization profile of structures described by Equation 4, with a variable coefficient a:

$$g(z) = \exp\left[-a\left(\frac{z-\frac{L}{2}}{L}\right)^2\right], \quad z \in [0, L], \tag{4}$$

Where g (z) is the approximation function, L is the lattice length.

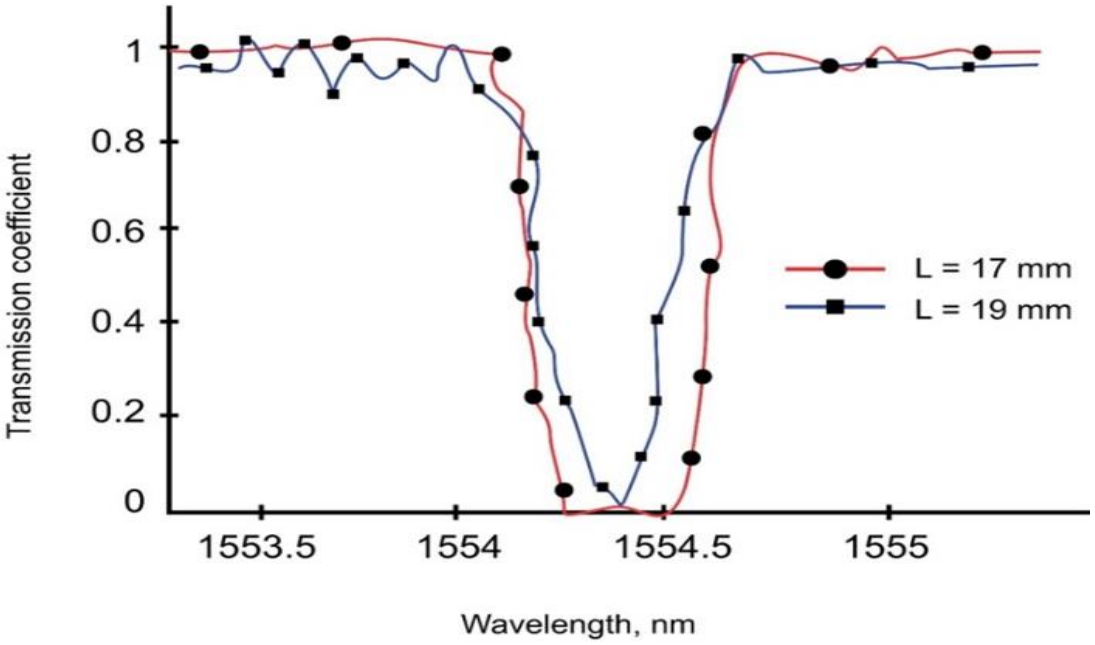

Figure 12.
FBG structure transfer in the absence of apodization for two selected lengths. Non-apodized structures.

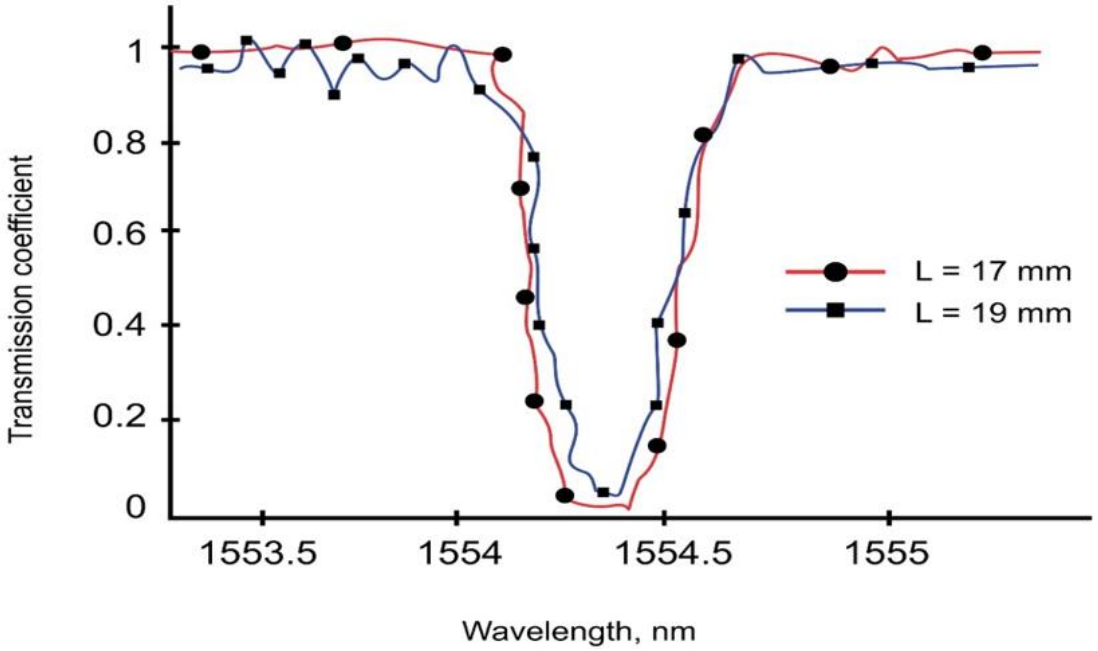

Figure 13.
Transfer of FBG structure during apodization for two selected structure lengths, apodized with a Gaussian profile with parameter value a = 15.

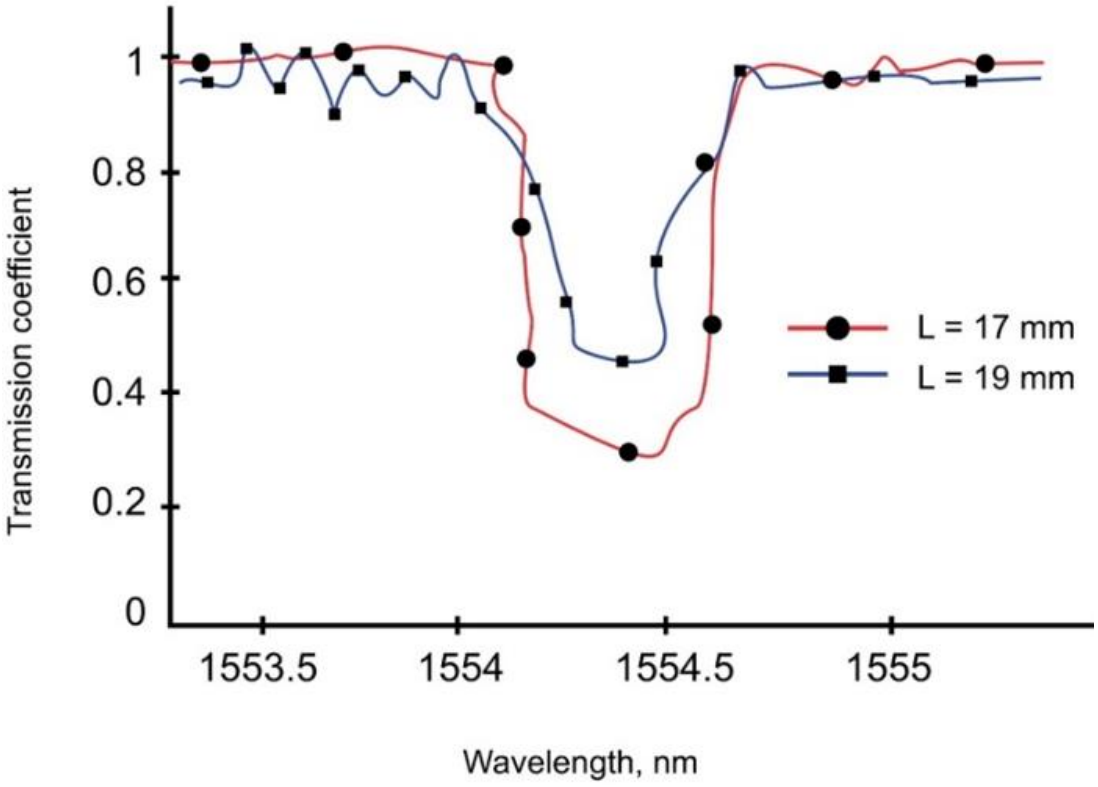

Figure 14.
Transfer of FBG structure during apodization for two selected structure lengths, apodized with a Gaussian profile with parameter value a = 200.

The types of periodic fiber-optic structures, their spectral properties, and the results of modeling the spectra of gratings with various technical parameters are presented, as well as the displacements of the central wavelengths of sensors built in the form of a network of sensors in various places on the plates. We used the transition matrix method to carry out numerical calculations of the spectral characteristics of Bragg gratings for variable physical parameters.

4. Conclusions

This paper presents experimental studies of fiber Bragg grating sensors embedded in the internal structure of composite plates. Analyzing the results, we see the impact of the refractive index modulation envelope that forms the FBG structure on its spectral characteristics. As you can see, changing parameter a Gaussian profile from a value of 15 to

a value of 200 leads to a decrease in the degree of so-called side bands in the spectral characteristics. However, it's important to note that the changes extend beyond just the sideband level. The greater the value of the parameter a, the greater the discrepancy in the signs of refraction of structures distinguished by real length. Thus, the more apodized the FBG structure, the more sensitive it is to changes in its length. The same change in the length of the structure, by 5 mm for a structure apodized with a profile with values of a = 15 and 200, is fundamentally different in the value of the transmission coefficient.

The work was supported by a grant and funding from the Ministry of Science and Higher Education of the Republic of Kazakhstan within the framework of the Project № AP19679153, Institute Information and Computational Technologies CS MSHE RK. Experimental research has been carried out in the laboratories of optoelectronics at the Electric Engineering and Computer Sciences faculty of Lublin Technical University.

References

[1] Y. Gebremichael *et al.*, "Integration and assessment of fibre Bragg grating sensors in an all-fibre reinforced polymer composite road bridge," *Sensors and Actuators A: Physical*, vol. 118, no. 1, pp. 78-85, 2005.

[2] M. Mieloszyk, K. Majewska, and W. Ostachowicz, "Application of embedded fibre Bragg grating sensors for structural health monitoring of complex composite structures for marine applications," *Marine Structures*, vol. 76, p. 102903, 2021. https://doi.org/10.1016/j.marstruc.2020.102903

[3] F. Cucinotta, E. Guglielmino, and F. Sfravara, "Life cycle assessment in yacht industry: A case study of comparison between hand lay-up and vacuum infusion," *Journal of Cleaner Production*, vol. 142, pp. 3822-3833, 2017. https://doi.org/10.1016/j.jclepro.2016.10.080

[4] Z. Liu *et al.*, "Reliability assessment of measurement accuracy for FBG sensors used in structural tests of the wind turbine blades based on strain transfer laws," *Engineering Failure Analysis*, vol. 112, p. 104506, 2020. https://doi.org/10.1016/j.engfailanal.2020.104506

[5] B. Wu, G. Wu, and C. Yang, "Parametric study of a rapid bridge assessment method using distributed macro-strain influence envelope line," *Mechanical Systems and Signal Processing*, vol. 120, pp. 642-663, 2019. https://doi.org/10.1016/j.ymssp.2018.10.039

[6] J. Chen, J. Wang, X. Li, L. Sun, S. Li, and A. Ding, "Monitoring of temperature and cure-induced strain gradient in laminated composite plate with FBG sensors," *Composite Structures*, vol. 242, p. 112168, 2020. https://doi.org/10.1016/j.compstruct.2020.112168

[7] T. Shafighfard, E. Demir, and M. Yildiz, "Design of fiber-reinforced variable-stiffness composites for different open-hole geometries with fiber continuity and curvature constraints," *Composite Structures*, vol. 226, p. 111280, 2019. https://doi.org/10.1016/j.compstruct.2019.111280

[8] P. Parandoush and D. Lin, "A review on additive manufacturing of polymer-fiber composites," *Composites Structure*, vol. 182, pp. 36-53, 2017.

[9] H. Guo, M. B. Gingerich, L. M. Headings, R. Hahnlen, and M. J. Dapino, "Joining of carbon fiber and aluminum using ultrasonic additive manufacturing (UAM)," *Composite Structures*, vol. 208, pp. 180-188, 2019. https://doi.org/10.1016/j.compstruct.2018.10.004

[10] T. Yu, Z. Zhang, S. Song, Y. Bai, and D. Wu, "Tensile and flexural behaviors of additively manufactured continuous carbon fiber-reinforced polymer composites," *Composite Structures*, vol. 225, p. 111147, 2019. https://doi.org/10.1016/j.compstruct.2019.111147

[11] N. Van De Werken, H. Tekinalp, P. Khanbolouki, S. Ozcan, A. Williams, and M. Tehrani, "Additively manufactured carbon fiber-reinforced composites: State of the art and perspective," *Additive Manufacturing*, vol. 31, p. 100962, 2020. https://doi.org/10.1016/j.addma.2019.100962

[12] S. Mahmood, A. Qureshi, and D. Talamona, "Taguchi based process optimization for dimension and tolerance control for fused deposition modelling," *Additive Manufacturing*, vol. 21, pp. 183-190, 2018. https://doi.org/10.1016/j.addma.2018.03.009

[13] P. K. Penumakala, J. Santo, and A. Thomas, "A critical review on the fused deposition modeling of thermoplastic polymer composites," *Composites Part B: Engineering*, vol. 201, p. 108336, 2020. https://doi.org/10.1016/j.compositesb.2020.108336

[14] S. Chakraborty and M. C. Biswas, "3D printing technology of polymer-fiber composites in textile and fashion industry: A potential roadmap of concept to consumer," *Composite Structures*, vol. 248, p. 112562, 2020. https://doi.org/10.1016/j.compstruct.2020.112562

[15] C. Kousiatza and D. Karalekas, "In-situ monitoring of strain and temperature distributions during fused deposition modeling process," *Materials and Design*, vol. 97, pp. 400-406, 2016.

[16] J.-Y. Lee, J. An, and C. K. Chua, "Fundamentals and applications of 3D printing for novel materials," *Applied Materials Today*, vol. 7, pp. 120-133, 2017. https://doi.org/10.1016/j.apmt.2017.02.004

[17] W. Zhong, F. Li, Z. Zhang, L. Song, and Z. Li, "Short fiber reinforced composites for fused deposition modeling," *Materials Science and Engineering: A*, vol. 301, no. 2, pp. 125-130, 2001. https://doi.org/10.1016/s0921-5093(00)01810-4

[18] F. Ning, W. Cong, J. Qiu, J. Wei, and S. Wang, "Additive manufacturing of carbon fiber reinforced thermoplastic composites using fused deposition modeling," *Composites Part B: Engineering*, vol. 80, pp. 369-378, 2015. https://doi.org/10.1016/j.compositesb.2015.06.013

[19] J. Chacón, M. Caminero, P. Núñez, E. García-Plaza, I. García-Moreno, and J. Reverte, "Additive manufacturing of continuous fibre reinforced thermoplastic composites using fused deposition modelling: Effect of process parameters on mechanical properties," *Composites Science and Technology*, vol. 181, p. 107688, 2019. https://doi.org/10.1016/j.compscitech.2019.107688

[20] S. F. Kabir, K. Mathur, and A.-F. M. Seyam, "A critical review on 3D printed continuous fiber-reinforced composites: History, mechanism, materials and properties," *Composite Structures*, vol. 232, p. 111476, 2020. https://doi.org/10.1016/j.compstruct.2019.111476

[21] M. Mieloszyk and W. Ostachowicz, "An application of structural health monitoring system based on FBG sensors to offshore wind turbine support structure model," *Marine Structures*, vol. 51, pp. 65-86, 2017. https://doi.org/10.1016/j.marstruc.2016.10.006

[22] C. Kousiatza, D. Tzetzis, and D. Karalekas, "In-situ characterization of 3D printed continuous fiber reinforced composites: A methodological study using fiber Bragg grating sensors," *Composites Science and Technology*, vol. 174, pp. 134-141, 2019. https://doi.org/10.1016/j.compscitech.2019.02.008

[23] L. Sorensen, J. Botsis, T. Gmür, and J. Cugnoni, "Delamination detection and characterisation of bridging tractions using long FBG optical sensors," *Composites Part A: Applied Science and Manufacturing*, vol. 38, no. 10, pp. 2087-2096, 2007. https://doi.org/10.1016/j.compositesa.2007.07.009

[24] M. Mieloszyk, A. Andrearczyk, K. Majewska, M. Jurek, and W. Ostachowicz, "Polymeric structure with embedded fiber Bragg grating sensor manufactured using multi-jet printing method," *Measurement*, vol. 166, p. 108229, 2020. https://doi.org/10.1016/j.measurement.2020.108229

[25] A. Fernández-Medina *et al.*, "Embedded fiber Bragg grating sensors for monitoring temperature and thermo-elastic deformations in a carbon fiber optical bench," *Sensors*, vol. 23, no. 14, p. 6499, 2023. https://doi.org/10.3390/s23146499

[26] M. Gabardi *et al.*, "Embedding fiber bragg grating sensors in carbon composite structures for accurate strain measurement," *IEEE Sensors Journal*, vol. 23, no. 15, pp. 16882-16892, 2023. https://doi.org/10.1109/jsen.2023.3285408

[27] B. Vedran, N. Matej, P. Simon, M. Boris, and D. Denis, "High-order fiber bragg grating corrosion sensor based on the detection of a local surface expansion," *Structural Control and Health Monitoring*, pp. 1-14, 2023.

[28] L. Shuochao, P. Zhu, F. Xie, and M. A. Soto, "Gecko-inspired self-adhesive packaging for strain-free temperature sensing based on optical fibre Bragg gratings," *Scientific Reports*, vol. 13, no. 1, pp. 1-10, 2023.

[29] A. Quattrocchi and R. Montanini, "Development and verification of self-sensing structures printed in additive manufacturing: A preliminary study," *Acta IMEKO*, vol. 12, no. 2, pp. 1-7, 2023. https://doi.org/10.21014/actaimeko.v12i2.1431